第 29 卷 第 5 期
2003 年 9 月

自 动 化 学 报
ACTA AUTOMATICA SINICA

Vol. 29, No. 5
Sept., 2003

Accurate Positioning in Real Time for Mobile Robot[1)]

XU De TAN Min

(*Laboratory of Complex Systems and Intelligence Science, Institute of Automation, Chinese Academy of Sciences, Beijing* 100080)

(E-mail: xude@compsys.ia.ac.cn)

Abstract The improvement of dead reckoning is presented. According to the movement trajectory and status of a mobile robot, a new kinematics model for the mobile robot is derived using coordinate transformation based on the turning radius and angle. And the turning radius and angle are obtained from the yawing angle information and the odometer information of the three wheels using fuzzy fusion technology. Combining the active beacon with improved dead reckoning, a new accurate positioning method for indoor mobile robot is proposed. The simulation shows that it has characteristics such as good performance in real time, high accuracy, low cost and good robustness. It is also suitable for rough ground.

Key words Mobile robot, positioning, kinematics, fuzzy fusion

1 Introduction

Localization is the foundation of mobile robots, and accurate localization in real time is a key factor to improve their performance, which is one of the research hotspots in the area of mobile robots. The methods of localization can be divided into two categories: the relative and the absolute. The relative methods, which are also called dead reckoning(DR), can be further divided into odometry and inertial navigation (IN). The absolute methods include global positioning system (GPS), active beacon (AB), magnetic compasses (MC), landmark navigation (LN) and map matching (MM)[1]. They have different characteristics, but only DR, AB, LN and MM are suitable for indoor mobile robots. Odometry, the representative of DR, is of great interest for its low cost and good performance in real time. It is common to combine DR with other absolute positioning methods for better positioning results through information fusion. This combination takes advantage of the high accuracy of positioning of DR in small range and the absolute methods in large range[2~5,11]. Lazea studied the kinematics and inverse kinematics models of mobile robots in 1996[6]. Chong and Kleeman presented a kind of DR to estimate position and orientation errors of a mobile robot by means of a statistical error model in 1997[7]. Borenstein and Feng provided a kind of systematic error verification method in 1996[8]. These methods have good performance in real time, but they are not suitable for the rough ground. Burgard proposed a position probability grid approach in 1996, which matches the local map against the global map to produce an absolute position and orientation estimate[9]. Roy and Thrun gave a statistical method for calibrating the odometry of a mobile robot with the help of an environment map in 1999[10]. El-Hakim presented a method of building the indoor 3-D map and a positioning approach using the map[11]. It has the advantage of positioning at a high accuracy, but has the disadvantage of high cost in calculation that makes the online robot move at a very low speed. Another weakness is it is easy to have mistake in characteristic matching.

Positioning accuracy of DR has important influence on the system performance. If the

1) Supported by China Postdoctoral Science Foundation and the National High Technology Research and Development Program of P. R. China(2001AA422170)
Received July 17, 2002; in revised form October 10, 2002
收稿日期 2002-07-17; 收修改稿日期 2002-10-10

absolute positioning method is failure, the system positioning accuracy will completely depend on DR. On the other hand, the information fusion of DR and absolute positioning method will involve iterative algorithm, in which the accuracy of DR will affect the speed of the algorithm by changing the iterative times. Therefore, it is very important to improve the positioning accuracy of DR, just as [1] points out that navigation tasks will be simplified and the performance of mobile robot will be improved if DR's accuracy is increased.

An improved DR method for mobile robot with redundant odometry information is proposed in this paper. Combining the active beacon with the improved DR, a new accurate real-time positioning method for indoor mobile robot is presented.

2 A new kind of kinematics model and DR with redundant information

The mobile robot concerned in this paper is of three wheels, as shown in Fig. 1. The front wheel is a guide wheel, the left rear wheel is a driving wheel, and the right rear wheel is a balance wheel. To reduce the influence of the slippage of the driving wheel on distance measurement while starting or braking, we refers to [7] and fix a measurement wheel driven by the friction of ground on the outside of the driving wheel. Three encoders are fixed on the measurement, balance and guide wheels, respectively, to measure the movement distance, as Encoder 1～3 in Fig. 1. Encoder 4 is fixed on the guide wheel for measuring its yawing angle. Encoder 4 is with absolute code, and the others with relative code.

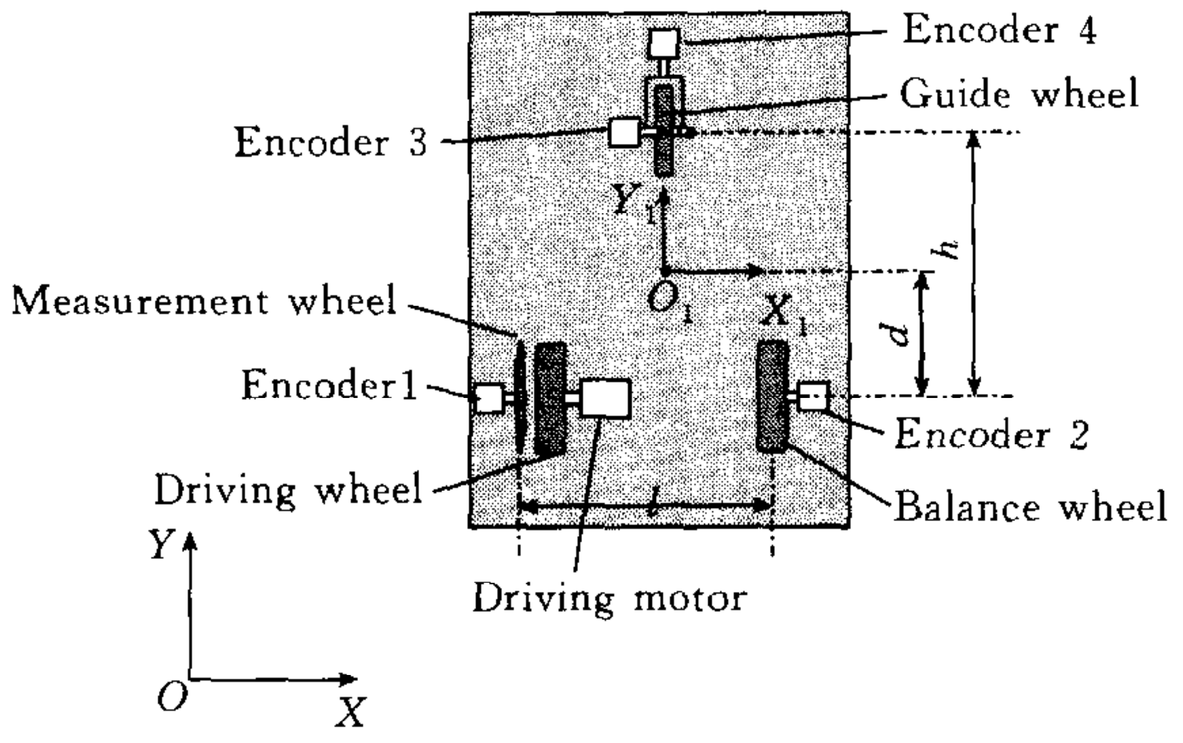

Fig. 1 The scheme of movement system for mobile robot with three wheels

In the following context, W_1, W_2 and W_3 denote the measurement, balance and guide wheels, respectively. O_1 is the geometric center of the robot. Let the distance between W_1 and W_2 be l, the perpendicular distance between W_3 and the line from W_1 to W_2 be h, and the perpendicular distance between O_1 and the line from W_1 to W_2 be d, respectively. Assume O_1, W_3 and the middle point of the line from W_1 to W_2 are on the perpendicular from W_3 to the line from W_1 to W_2.

XOY is the base coordinates, and $X_1O_1Y_1$ is the robot coordinates. The direction of $\boldsymbol{Y}_1$ is from O_1 to W_3. S_j^{ii+1} indicates the distance that W_j moves in the interval between the i-th and the $i+1$-th sampling, the direction of $\boldsymbol{Y}_1$ presents the positive direction of S_j^{ii+1}.

We describe the position and pose of the robot as T_{O1}^i using a 3×3 homogeneous matrix:

$$T_{O_1}^i = \begin{bmatrix} m_x^i & n_x^i & p_x^i \\ m_y^i & n_y^i & p_y^i \\ 0 & 0 & 1 \end{bmatrix} \tag{1}$$

where $m_x^i i + m_y^i j$ is the representation of $\boldsymbol{X}_1$ in XOY coordinates, $n_x^i i + n_y^i j$ is the representation of $\boldsymbol{Y}_1$ in XOY coordinates, and (p_x^i, p_y^i) is the position of O_1 in XOY coordinates.

2.1 Kinematics model based on movement trajectory

The movement trajectory of the mobile robot can be described as line and circular arc. Its position and direction can be derived from the movement distance when it moves in line, or from arc radius and central angle when it moves in arc. The arc radius and central angle come from the 4 encoders through information fusion. We will discuss how to get them in Section 2.2 and consider them as known parameters for the time being.

2.1.1 The robot moves in line

When the robot moves in line, it moves in the direction of $\boldsymbol{Y}_1$. We have $S_1^{ii+1} = S_2^{ii+1} = S_3^{ii+1}$ and $\alpha^i = 0$, where α^i is the yawing angle of W_3. $T_{O_1}^{i+1}$, which is the position and pose of point O_1 at the $i+1$-th sampling, can be obtained through translation transformation:

$$T_{O_1}^{i+1} = \begin{bmatrix} m_x^i & n_x^i & p_x^i + S_1^{ii+1} n_x^i \\ m_y^i & n_y^i & p_y^i + S_1^{ii+1} n_y^i \\ 0 & 0 & 1 \end{bmatrix} \tag{2}$$

2.2.2 The robot moves in circular arc

When the robot moves in circular arc, the central point O_2 of the circular arc can be taken as a rotation joint. The directions of $\boldsymbol{X}_2$ and $\boldsymbol{Y}_2$ are defined as these of $\boldsymbol{X}_1$ and $\boldsymbol{Y}_1$, shown in Fig. 2. We can get $T_{O_2}^i$ from $T_{O_1}^i$ through translation transformation, $T_{O_2}^{i+1}$ from $T_{O_2}^i$ through rotation transformation, and $T_{O_1}^{i+1}$ from $T_{O_2}^{i+1}$ through translation transformation. $T_{O_2}^i$ and $T_{O_2}^{i+1}$ are the position and pose of point O_1 at the i-th and $i+1$-th sampling, respectively.

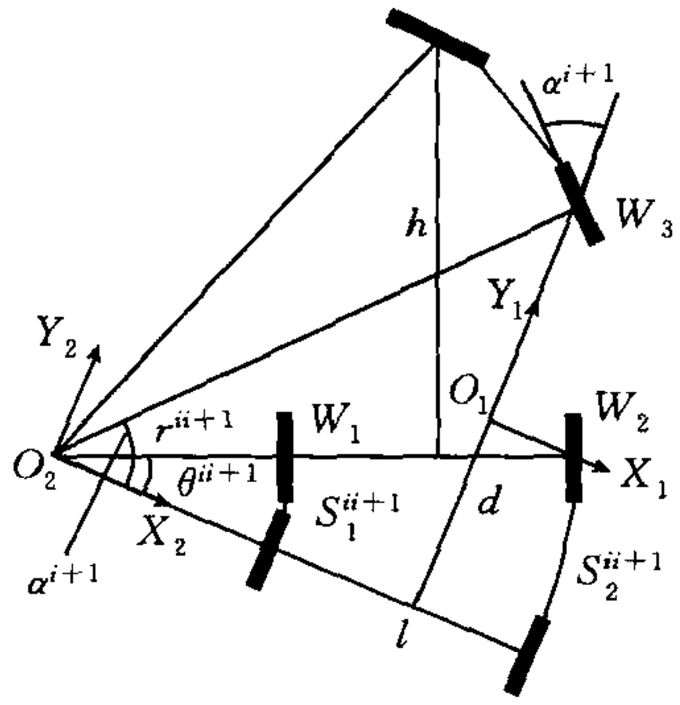

Fig. 2 The diagram of curve trajectory

$$\begin{aligned} T_{O_1}^{i+1} &= T_{O_1}^i \, Trans(-r^{ii+1} - l/2, -d) \, Rot(\theta^{ii+1}) \, Trans(r^{ii+1} + l/2, d) \\ &= \begin{bmatrix} m_x^i & n_x^i & p_x^i \\ m_y^i & n_y^i & p_y^i \\ 0 & 0 & 1 \end{bmatrix} \begin{bmatrix} 1 & 0 & -r^{ii+1} - l/2 \\ 0 & 1 & -d \\ 0 & 0 & 1 \end{bmatrix} \begin{bmatrix} c\theta^{ii+1} & -s\theta^{ii+1} & 0 \\ s\theta^{ii+1} & c\theta^{ii+1} & 0 \\ 0 & 0 & 1 \end{bmatrix} \begin{bmatrix} 1 & 0 & r^{ii+1} + l/2 \\ 0 & 1 & d \\ 0 & 0 & 1 \end{bmatrix} \\ &= \begin{bmatrix} m_x^i c\theta^{ii+1} + n_x^i s\theta^{ii+1} & -m_x^i s\theta^{ii+1} + n_x^i c\theta^{ii+1} & \begin{array}{c}(m_x^i c\theta^{ii+1} + n_x^i s\theta^{ii+1} - m_x^i)(r^{ii+1} + l/2) \\ -(m_x^i s\theta^{ii+1} - n_x^i c\theta + n_x^i)d + p_x^i\end{array} \\ m_y^i c\theta^{ii+1} + n_y^i s\theta^{ii+1} & -m_y^i s\theta^{ii+1} + n_y^i c\theta^{ii+1} & \begin{array}{c}(m_y^i c\theta^{ii+1} + n_y^i s\theta^{ii+1} - m_y^i)(r^{ii+1} + l/2) \\ -(m_y^i s\theta^{ii+1} - n_y^i c\theta + n_y^i)d + p_y^i\end{array} \\ 0 & 0 & 1 \end{bmatrix} \end{aligned} \tag{3}$$

where r^{ii+1} is the x-coordinate of the intersection of the trajectory of W_1 with the X_2 coordinate in the interval of the i-th and the $i+1$-th sampling; θ^{ii+1} is the central angle of circu-

lar arc in that interval.

2.2 The methods of calculation r^{ii+1} and θ^{ii+1}

We use α^i to denote the yawing angle of W_3 at the i-th sampling and define its positive direction as counterclockwise in the bird's eye view. r^{ii+1} and θ^{ii+1} can be obtained from any two parameters in the group of S_1^{ii+1}, S_2^{ii+1}, S_3^{ii+1} and α^i. The values of r^{ii+1} and θ^{ii+1} obtained from different parameters are different because of the influence of uneven ground and measurement noise. It is easy to get 6 groups of r^{ii+1} and θ^{ii+1} according to the geometry relation in Fig. 2.

To reduce the influence of random factors and get accurate values of r^{ii+1} and θ^{ii+1}, we form their estimated values through fusion of 6 groups of r^{ii+1} and θ^{ii+1}. There are 6 different values of θ^{ii+1} and 4 different values of r^{ii+1} in the 6 groups. So we fuse r^{ii+1} and θ^{ii+1} separatively. Generally, random errors submit to normal distribution. Therefore, a kind of exponential function similar to normal distribution function is employed as membership function as follows:

$$\begin{cases} \mu_{\tilde{r}}(r_j) = k_{rj} \cdot \mathrm{e}^{-\frac{(r_j-\bar{r})^2}{\sigma_r^2}} \\ \mu_{\tilde{\theta}}(\theta_j) = k_{\theta j} \cdot \mathrm{e}^{-\frac{(\theta_j-\bar{\theta})^2}{\sigma_\theta^2}} \end{cases} \tag{4}$$

where $\bar{r} = \dfrac{\sum_{j=1}^{m} r_j}{m}, \bar{\theta} = \dfrac{\sum_{j=1}^{n} \theta_j}{n}$, $m=4$, and $n=6$. $\tilde{r}$ and $\tilde{\theta}$ are fuzzy set. σ_r and σ_θ are distributive parameters, and are assigned by (5). k_{rj} and $k_{\theta j}$ are power factors representing the *concentrative* degrees of r_j and θ_j, and are shown in (6) and (7).

$$\begin{cases} \sigma_r = \dfrac{1}{4} \left| \max\{r_1 \sim r_4\} - \min\{r_1 \sim r_4\} \right| \\ \sigma_\theta = \dfrac{1}{4} \left| \max\{\theta_1 \sim \theta_6\} - \min\{\theta_1 \sim \theta_6\} \right| \end{cases} \tag{5}$$

$$\begin{cases} k_{rj} = \sum_{l=1}^{4} k_{rjl} \\ k_{\theta j} = \sum_{l=1}^{6} k_{\theta jl} \end{cases} \tag{6}$$

$$k_{rjl} = \begin{cases} 1, & |r_j - r_l| < \sigma_r \\ 0, & \text{others} \end{cases}, \quad k_{\theta jl} = \begin{cases} 1, & |\theta_j - \theta_l| < \sigma_\theta \\ 0, & \text{others} \end{cases} \tag{7}$$

The estimated values of r^{ii+1} and θ^{ii+1} are calculated by (8) using Takagi-Sugeno fuzzy algorithm.

$$\hat{r}^{ii+1} = \frac{\sum_{j=1}^{m} \mu_{\tilde{r}}(r_j) r_j}{\sum_{j=1}^{m} \mu_{\tilde{r}}(r_j)}, \quad \hat{\theta}^{ii+1} = \frac{\sum_{j=1}^{n} \mu_{\tilde{\theta}}(\theta_j) \theta_j}{\sum_{j=1}^{n} \mu_{\tilde{\theta}}(\theta_j)} \tag{8}$$

Then we compare $\hat{r}^{ii+1}$ and $\hat{\theta}^{ii+1}$ them with $\bar{r}$ and $\bar{\theta}$, respectively. If $|\hat{r}^{ii+1} - \bar{r}| < 0.1\text{mm}$ and $|\hat{\theta}^{ii+1} - \bar{\theta}| < 0.00001\text{rad}$, then we take $\hat{r}^{ii+1}$ and $\hat{\theta}^{ii+1}$. Otherwise, let $\bar{r} = \hat{r}^{ii+1}$ and $\bar{\theta} = \hat{\theta}^{ii+1}$, and recalculate $\hat{r}^{ii+1}$ and $\hat{\theta}^{ii+1}$ using (4~8). The times of recalculation is limited to 5.

3 A new positioning method combining DR with AB

Ghidary[12] presented a kind of indoor AB positioning method in 1999. Its principle is as follows: The emitter in the mobile robot sends ultrasonic and infrared signals at the

same time. When the receiving device in the room receives the infrared signal, it triggers the timer to start timing. When it receives the ultrasonic signal, it stops timing. Then the transmission time of the ultrasonic signal is obtained. And the distance from the receiver to the robot can be calculated from the time. The localization of the robot can be realized by means of the distances from three receivers to the robot. The emitter consists of 8 infrared emitters and 8 ultrasonic emitters. The receiver consists of 3 infrared receivers and 3 ultrasonic receivers. There exists a blind area in the receiving device. So six sets of receiver device are mounted in a room sized 6×4m to ensure at least three sets can receive signals at the same time. It makes a high cost. In addition, the movement of the robot is controlled by a slave computer, and the positioning is realized in a master computers. The master and slave computers communicate to exchange information. It makes a large delay in position closed loop system. The method fails when the infrared signal is sheltered, as often seen in the indoor environment where human coexist with robot.

To overcome the disadvantage that the positioning and the movement control don't work in the same computer and reduce cost, we propose a new scheme shown in Fig. 3(a). A radio emitter and 2 ultrasonic receivers are mounted on the robot. A radio receiver and ultrasonic emitters are fixed on the ceiling. The radio pulse signal is used to trigger ultrasonic emitters and start two timers in the robot. When ultrasonic receivers receive the ultrasonic signal, they stop the timers respectively. Then the transmission time of the ultrasonic signal from emitter to 2 receivers can be obtained. The distances from emitter to 2 receivers can be respectively calculated from the time. Considering that DR has high accuracy in short term, we propose a new positioning method combining DR with AB, which employs the improved DR in Section 2 as main positioning method and AB as online revision method.

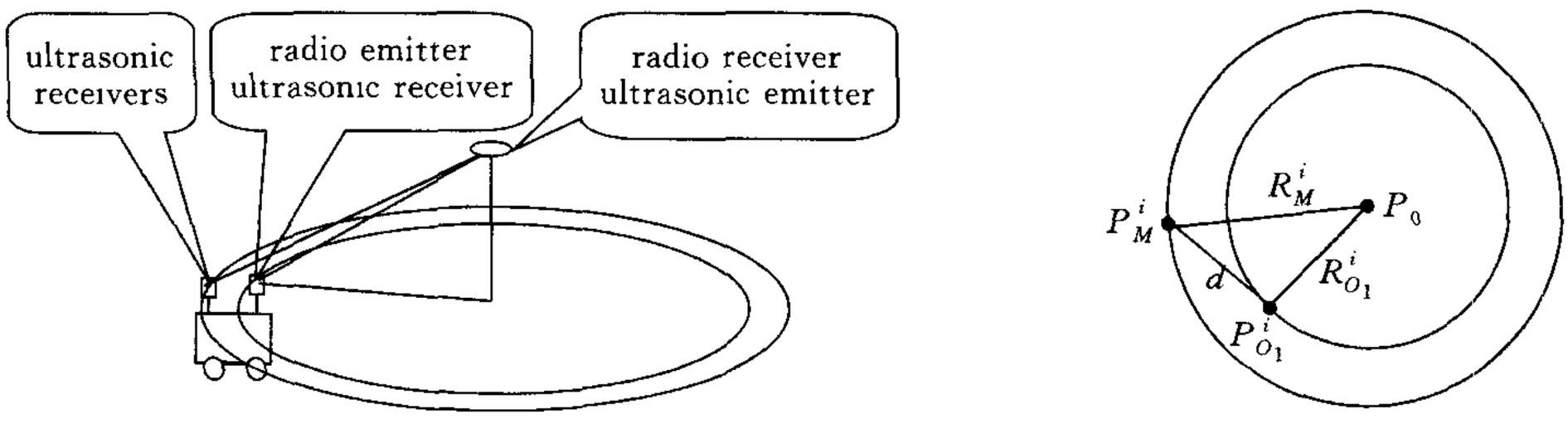

(a) The scheme of AB distance measuring (b) The position revision

Fig. 3 The scheme of the positioning method combining DR with AB

To simplify calculation, we fix one ultrasonic receiver at the geometric center point O_1 of the robot and the other at the middle point M of the line from W_1 to W_2. We denote the projection position of ultrasonic emitter to ground as P_0, the distance calculated at the i-th sampling from P_0 to O_1 as $R_{O_1}^i$, from P_0 to M as R_M^i, the position of O_1 as $P_{O_1}^i$ and the position of M as P_M^i. It is easy to work out $R_{O_1}^i$ and R_M^i in high accuracy by means of the distances from the ultrasonic emitter to O_1 and M. Therefore, we can revise $P_{O_1}^i$ to improve the positioning accuracy by means of $d, R_{O_1}^i$, R_M^i and P_0.

The three sides of the triangle formed by points $P_0, P_{O_1}^i$ and P_M^i are known in Fig. 3 (b). The angle between $R_{O_1}^i$ and R_M^i can be obtained as follows:

$$\gamma = \arccos[(R_{O_1}^{i\,2} + R_M^{i\,2} - d^2)/(2R_{O_1}^i R_M^i)] \tag{9}$$

$\hat{P}_M^i$ indicates revised P_M^i. $\hat{\beta}_M^j$ indicates the direction angle from $\hat{P}_M^i$ to P_0. $\hat{P}_{O_1}^i$ denotes revised $P_{O_1}^i$. $\hat{\beta}_{O_1}^j$ denotes the direction angle from $\hat{P}_{O_1}^i$ to P_0. Symbol j represents the itera-

tive times to calculate $\hat{\beta}_M^i$. We have:

$$\hat{\beta}_{O_1}^i = \hat{\beta}_M^i \pm \gamma \tag{10}$$

$$\begin{cases} \hat{p}_{Mx}^i = p_{0x} + R_M^i \cos\hat{\beta}_M^i \\ \hat{p}_{My}^i = p_{0y} + R_M^i \sin\hat{\beta}_M^i \end{cases} \tag{11}$$

$$\begin{cases} \hat{p}_{O_1x}^i = p_{0x} + R_{O_1}^i \cos\hat{\beta}_{O_1}^i \\ \hat{p}_{O_1y}^i = p_{0y} + R_{O_1}^i \sin\hat{\beta}_{O_1}^i \end{cases} \tag{12}$$

where p_{0x} and p_{0y} are the coordinates of point P_0. γ is an unsigned number, its range is in $[0, \pi]$. (10) shows that $\hat{\beta}_{O_1}^i$ has two possible values, but its real value must be one of them.

Obviously, the revision of P_M^i and $P_{O_1}^i$ can be done after getting $\hat{\beta}_M^i$. For getting $\hat{\beta}_M^i$, the target function is configured using the distances from P_M^i to $\hat{P}_M^i$ and from $P_{O_1}^i$ to $\hat{P}_{O_1}^i$, as shown in (13). In the condition of keeping the triangle shape in Fig. 3(b), we use the target function to explore in the circles whose radii are R_M^i and $R_{O_1}^i$ the points that are nearest to P_M^i and $P_{O_1}^i$, i. e., $\hat{P}_M^i$ and $\hat{P}_{O_1}^i$.

$$E = \frac{1}{2}[(\hat{p}_{Mx}^i - p_{Mx}^i)^2 + (\hat{p}_{My}^i - p_{My}^i)^2 + (\hat{p}_{O_1x}^i - p_{O_1x}^i)^2 + (\hat{p}_{O_1y}^i - p_{O_1y}^i)^2] \tag{13}$$

Differentiating E with respect to $\hat{\beta}_M^i$, we have

$$\frac{dE}{d\hat{\beta}_M^i} = -R_M^i(\hat{p}_{Mx}^i - p_{Mx}^i)\sin\hat{\beta}_M^i + R_M^i(\hat{p}_{My}^i - p_{My}^i)\cos\hat{\beta}_M^i - R_{O_1}^i(\hat{p}_{O_1x}^i - p_{O_1x}^i)\sin\hat{\beta}_{O_1}^i + R_{O_1}^i(\hat{p}_{O_1y}^i - p_{O_1y}^i)\cos\hat{\beta}_{O_1}^i \tag{14}$$

Take the direction of gradient descend as the search direction of $\hat{\beta}_M^i$. $\hat{\beta}_M^{ij+1}$, the increment of $\hat{\beta}_M^i$, is as follows:

$$\hat{\beta}_M^{ij+1} = -\frac{k}{R_M^i R_{O_1}^i} \cdot \frac{dE}{d\hat{\beta}_M^i} \tag{15}$$

where k is the step factor, and $k=0.5$.

$$\hat{\beta}_M^{i+1} = \hat{\beta}_M^i + \hat{\beta}_M^{ij+1} \tag{16}$$

In addition, $\hat{\beta}_M^0$, i. e., the initial value of $\hat{\beta}_M^i$, is defined as the direction angle from P_M^i to P_0.

$$\hat{\beta}_M^0 = \text{atan2}(p_{My}^i - p_{0y}, p_{Mx}^i - p_{0x}) \tag{17}$$

It is difficult to determine which of the two possible values of $\hat{\beta}_{O_1}^i$ should be available in the process of calculating. So we configure two target functions E_1 and E_2 using (13) corresponding to the two possible values. We can get $\hat{\beta}_{M1}^i$ and $\hat{\beta}_{M2}^i$ which make E_1 and E_2 take minimal values using iterative algorithm. If $E_1 < E_2$, then take $\hat{\beta}_{M1}^i$ as $\hat{\beta}_M^i$. Otherwise, take $\hat{\beta}_{M2}^i$ as $\hat{\beta}_M^i$. The coordinates of $\hat{P}_M^i$ and $\hat{P}_{O_1}^i$ can be calculated from (11), (12) using $\hat{\beta}_M^i$, and the modification of the positions of P_M^i and $P_{O_1}^i$ can be realized. σ, the direction angle from $\hat{P}_M^i$ to $\hat{P}_{O_1}^i$, can be obtained from the coordinates of $\hat{P}_M^i$ and $\hat{P}_{O_1}^i$. Then the modification of the robot's direction is realized:

$$\sigma = \text{atan2}(\hat{p}_{O_1y}^i - \hat{p}_{My}^i, \hat{p}_{O_1x}^i - \hat{p}_{Mx}^i) \tag{18}$$

$$\hat{T}_{O_1}^i = \begin{bmatrix} \cos\sigma & -\sin\sigma & \hat{p}_{O_1x}^i \\ \sin\sigma & \cos\sigma & \hat{p}_{O_1y}^i \\ 0 & 0 & 1 \end{bmatrix} \tag{19}$$

4 Simulation and results

The parameters of the mobile robot with three wheels are assumed as follows: $l=600$mm, $d=400$mm, $h=800$mm. The reference trajectory of point O_1 is selected as a circle centered at (4000mm, 4000mm)and with a radius of 2000mm. The movement step length of point O_1 is chosen as one-thousandth the circle perimeter. The coordinates of $W_1 \sim W_3$ and the yawing angle of W_3 can be calculated accurately using the reference trajectory of O_1 and

the step. They are taken as the measurement data after adding bounded random data with zero mean to them:

$$D_m = D_a(1 + 0.1D_d) \tag{20}$$

where D_m is measurement data, D_a is accurate data, D_d is bounded random data.

In addition, we have the data formed in (21) as a pothole in the path. $D_m + D_p$ denotes the measurement data when one wheel go across the pothole.

$$D_p = 5\sin(\pi i/50), \quad i = 0,1,\cdots,50 \tag{21}$$

where D_p is the pothole data.

In simulation, when the yawing angle is less than 0.01rad and the average of $S_1^{ü+1}$ and $S_2^{ü+1}$ is greater than 5mm, or the turning radius is greater than 100,000mm and the average of $S_1^{ü+1}$ and $S_2^{ü+1}$ is less than 30mm, we take the movement trajectory of the robot as line.

4.1 Simulation of the improved DR

Fig. 4 shows the simulation results of the improved DR and general DR. Fig. 4(a) and Fig. 4 (b) are the simulation results without the pothole in the path. Fig. 4(a) is the result using the method of improved DR in Section 2. The distance from the ending point of the simulation result to that of the reference is 43mm. Fig. 4(b) is the result using the general DR. The distance from the ending point of the simulation result to that of the reference is 150mm.

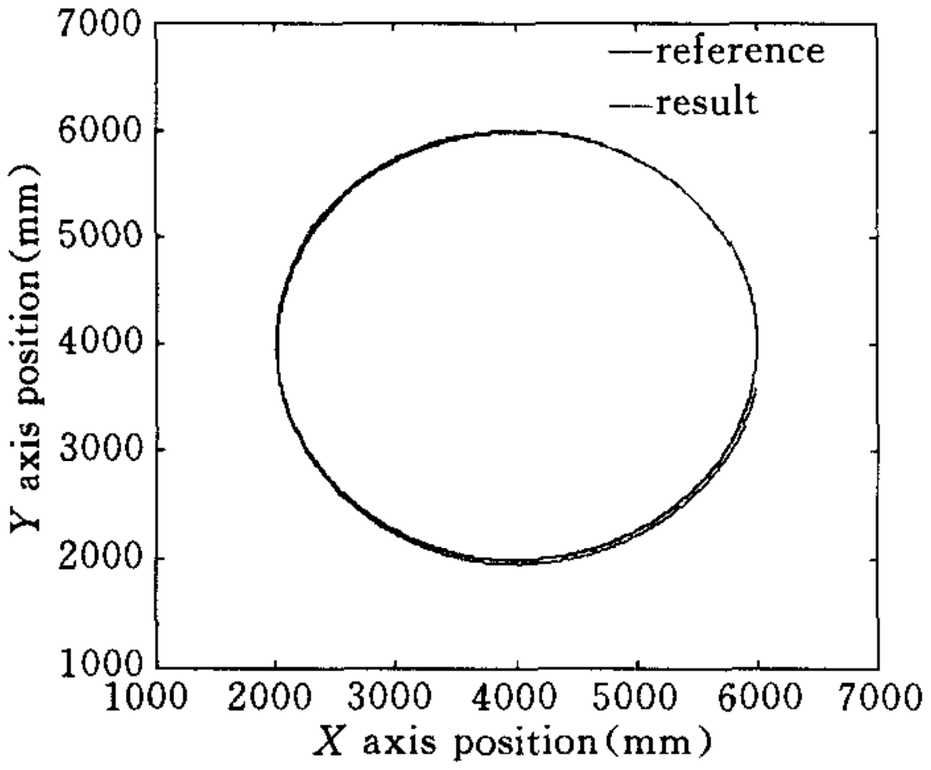

(a) The result obtained from the data of $W_1 \sim W_3$

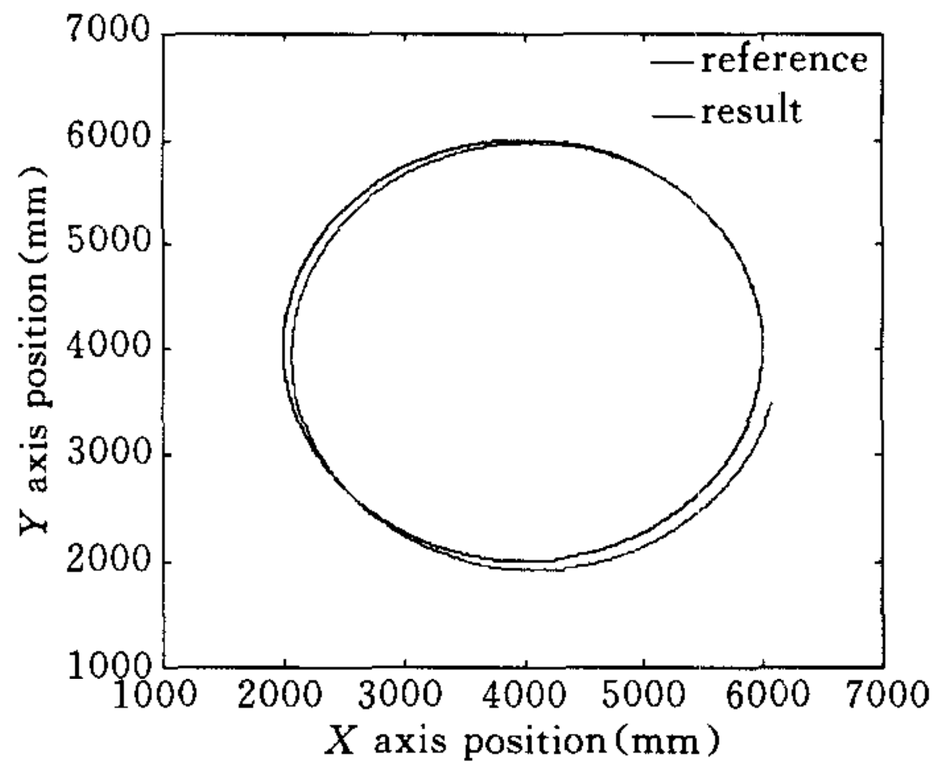

(b) The result obtained from the data of W_1 and W_2

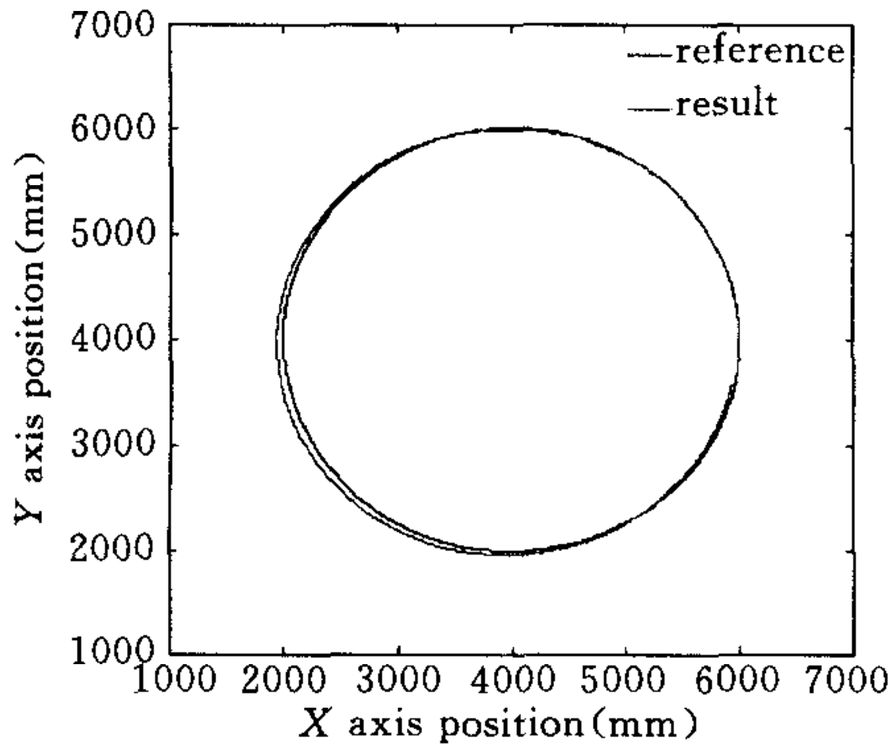

(c) The result obtained from the data of $W_1 \sim W_3$ when there is a pothole in the moving path of W_1

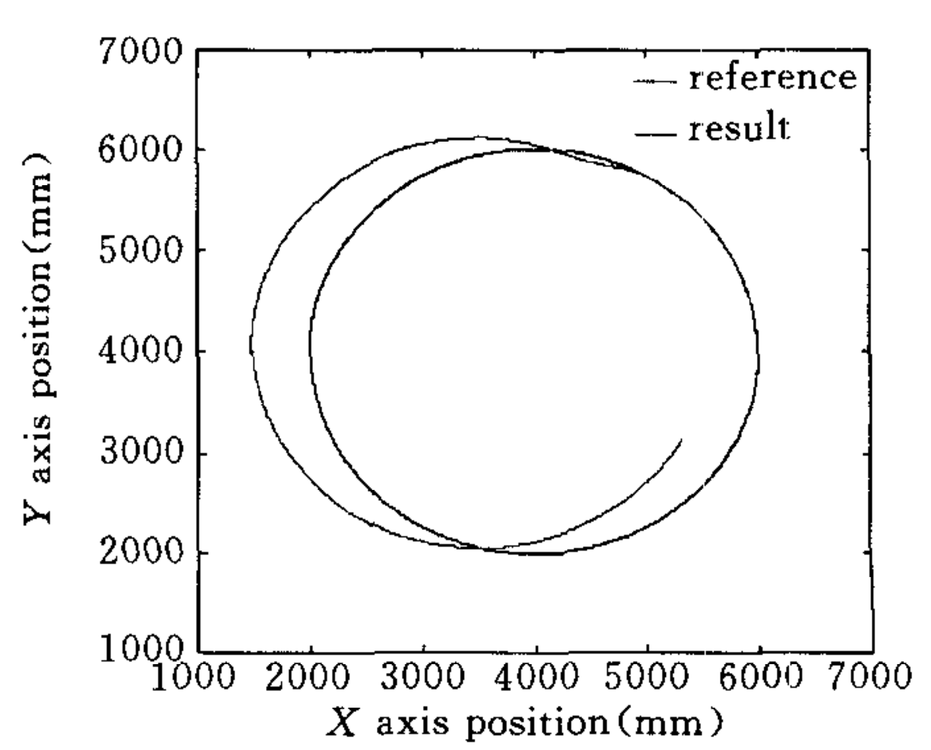

(d) The result obtained from the data of W_1 and W_2 when there is a pothole in the moving path of W_1

Fig. 4 The simulation results of DR

Values for the position and pose of O_1 at the ending points of the reference trajectory, improved DR and general DR are as follows.

$$\begin{bmatrix} 1 & 0 & 5959.6 \\ 0 & 1 & 3600.0 \\ 0 & 0 & 1 \end{bmatrix}, \quad \begin{bmatrix} 1 & 0 & 5990.3 \\ 0 & 1 & 3569.8 \\ 0 & 0 & 1 \end{bmatrix}, \quad \begin{bmatrix} 1 & 0 & 6077.7 \\ 0 & 1 & 3507.2 \\ 0 & 0 & 1 \end{bmatrix}$$

Fig. 4(c) and Fig. 4(d) are the simulation results with the pothole in the moving path of wheel W_1. The results are omitted because they are similar to those in Fig. 4(c) and Fig. 4(d) if there is a pothole in the moving path of wheel W_2 or W_3. In simulation, the data of the pothole are added to the data of the wheel from step 200.

From Fig. 4, we can find that the ability of eliminating the influence of random noise is better for the improved DR method than for the general method. The positioning accuracy of the improved DR is much higher than that of the general DR.

4.2 Simulation of the positioning method combining the improved DR with AB

In the simulation of the positioning method combining the improved DR with AB, we employ the improved DR as the main positioning method and AB as a revision online method. The position and pose of the mobile robot are modified once every ten steps. The data of the pothole are added to the data of wheel W_1 from step 200 on. Fig. 5(a) is the result using the method combining the improved DR with AB. The distance from the ending point of the simulation result to that of the reference is 0.94mm. Fig. 5(b) is the result using the method combining general DR with AB. The distance from the ending point of the simulation result to that of the reference is 65.33mm.

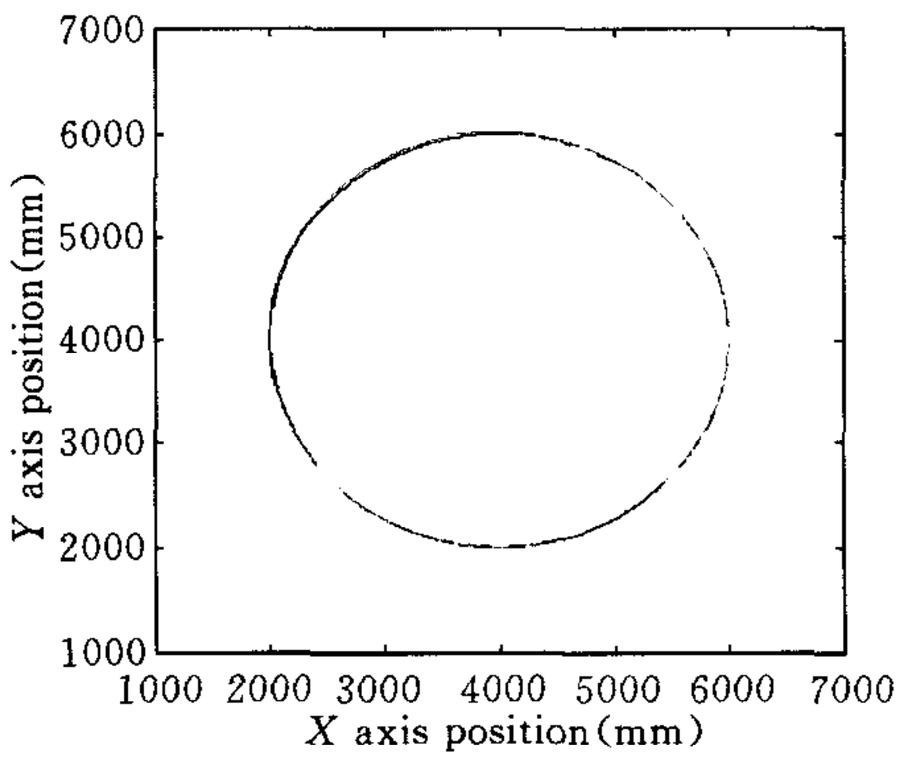

(a) The result of the method combining improved DR with AB

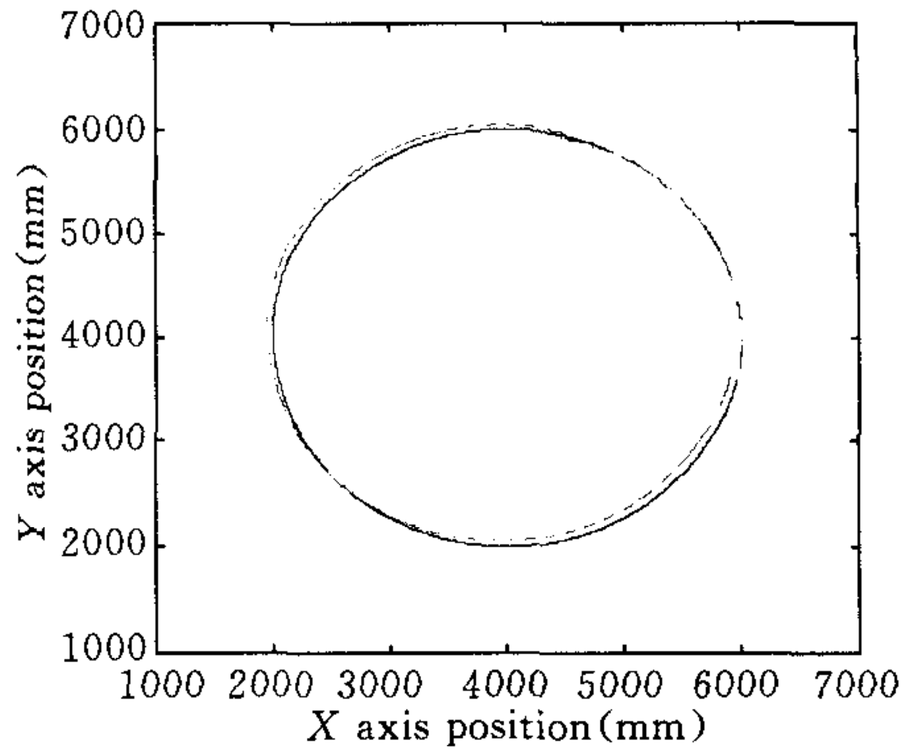

(b) The result of the method combining general DR with AB

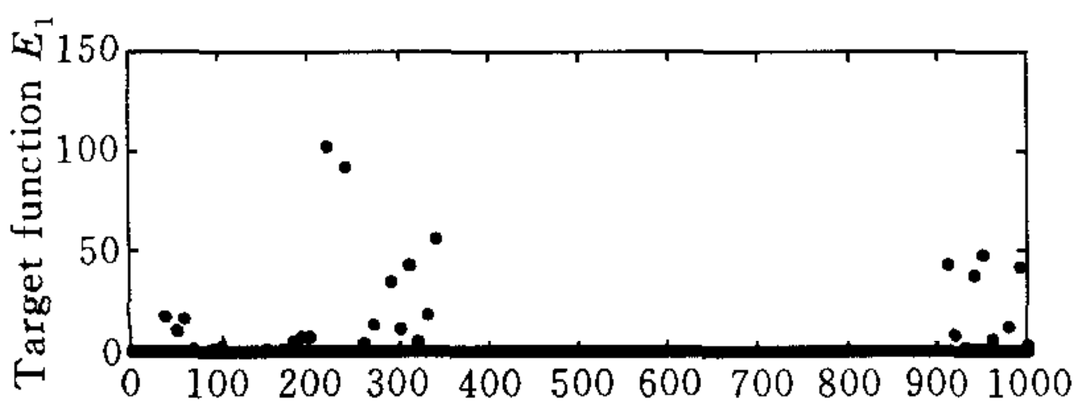

(c) Target function E_1

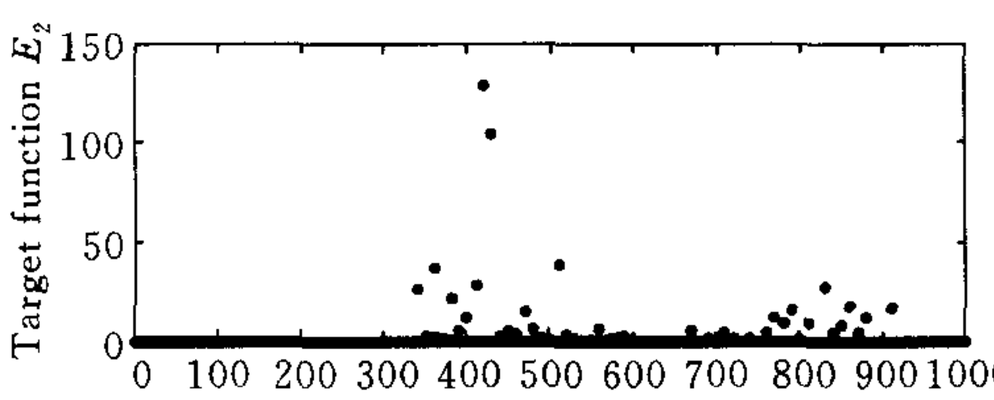

(d) Target function E_2

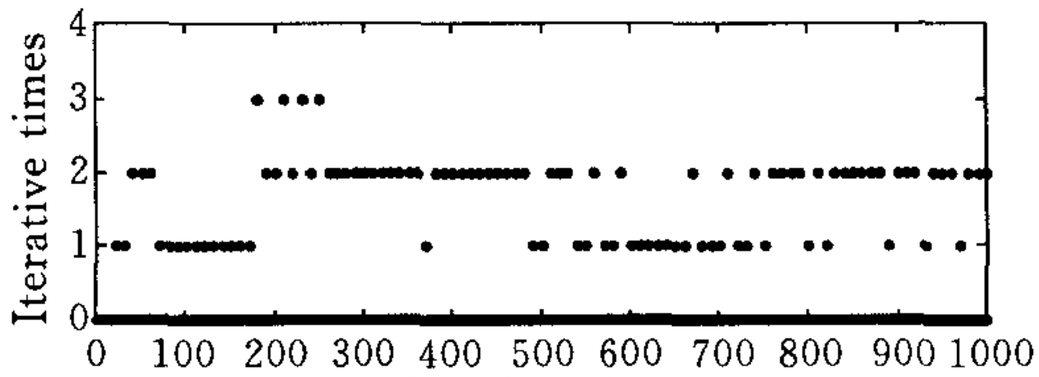

(e) Iterative times

Fig. 5 The simulation results of the method combining DR with AB

Values for the position and pose of O_1 at the ending points of the reference trajectory, improved DR with AB, and general DR with AB are as follows:

$$\begin{bmatrix} 1 & 0 & 5959.6 \\ 0 & 1 & 3600.0 \\ 0 & 0 & 1 \end{bmatrix}, \quad \begin{bmatrix} 1 & 0 & 5960.4 \\ 0 & 1 & 3599.5 \\ 0 & 0 & 1 \end{bmatrix}, \quad \begin{bmatrix} 1 & 0 & 5904.5 \\ 0 & 1 & 3635.1 \\ 0 & 0 & 1 \end{bmatrix}$$

The result of target function E_1 is shown in Fig. 5(c), E_2 in Fig. 5(d). Fig. 5(e) is the iterative times using AB to modify the position and pose of the mobile robot online. We can find from Fig. 5(e) that the number of iterative times is very little. This means that the iterative algorithm has high convergence speed and good performance in real time.

5 Conclusion

A new kind of kinematics model based on movement trajectory for mobile robot is deduced through the analysis of the status and movement trajectory in this paper. It gives the information of movement trajectory, i. e., the turning radius and angle, through information fuzzy fusion using the odometer information of three wheels and the yawing angle of the guide wheel. Then it provides the position and pose of the mobile robot by means of the kinematics model. Combining the improved DR method with AB, a new accurate positioning method in real time for indoor mobile robot is presented. The simulation confirms the effectiveness of this method.

The method has the characteristics as follows.

1) It is suitable for rough ground.

2) It has good performance in real time. It can meet the need of online positioning when the mobile robot moves quickly.

3) It has high positioning accuracy. In simulation, the data of each wheel are added random noise with zero mean and variance of 0.2 according to (20). The data of the pothole are added to the measure data of wheel W_1 from step 200 on according to (21). The mobile robot moves one perimeter on the circle whose radius is 2,000mm. The positioning error is only 0.94mm.

4) It is robust. It has very good ability of resisting disturbance.

5) It only needs present data to realize the modification of the position and pose of the robot online.

6) Temporary shelter of ultrasonic signals has weak influence on the positioning accuracy.

7) Its cost is low. Comparing with the scheme in [12], the cost is reduced obviously.

References

1 Borenstein J, Everett H R, Feng L, Wehe D. Mobile robot positioning: Sensors and techniques. *Journal of Robotic Systems*, 1997, **14**(4): 231～249

2 Thrapp R, Westbrook C, Subramanian D. Robust localization algorithms for an autonomous campus tour guide. In: Proceedings of the IEEE International Conference on Robotics & Automation, Seoul: IEEE Press, 2001. 2065～2071

3 Bonnifait Ph, Garcia G. Design and experimental validation of an odometric and goniometric localization system for outdoor robot vehicles. *IEEE Transactions on Robotics and Automation*, 1998, **14**(4): 541～548

4 Kleeman L. Optimal estimation of position and heading for mobile robots using ultrasonic beacons and dead-reckoning. In: IEEE International Conference on Robotics and Automation, Nice: IEEE Press, 1992, 2582～2587

5 Chong K S, Kleeman L. Feature-based mapping in real, large scale environments using an ultrasonic array. *International Journal Robotics Research*, 1999, **18**(1): 3～19

6 Lazea Gh, Lupu E, Patko M. Aspects on kinematic modelling and simulation of wheeled robots. International Symposium on Systems Theory, Robotics, Computers and Process Informatics, SINTES 8, Craiova: University of Craiova Press, 1996. 150～156

7 Chong K S, Kleeman L. Accurate odometry and error modelling for a mobile robot. In: Proceedings of IEEE International Conference on Robotics and Automation, New Mexico: IEEE Press, 1997. 2783～2788

8 Borenstein J, Feng L. Measurement and correction of systematic odometry errors in mobile robots. *IEEE Transactions on Robotics and Automation*, 1996, **12**(6):869～880

9 Burgard W, Fox D, Hennig D, Schmidt T. Estimating the absolute position of a mobile robot using position probability grids. In: Proceedings of the 13th National Conference on Artificial Intelligence(AAAI), Portland, AAAI Press, 1996, 896～901

10 Roy N, Thrun S. Online self-calibration for mobile robots. In: IEEE International Conference on Robotics and Automation, Detroit, IEEE Press, 1999, 2292～2297

11 El-Hakim S F, Boulanger P, Blais F, Beraldin J-A, Roth G. A mobile system for indoors 3-D mapping and positioning. In: Optical 3-D Measurement Techniques(IV), Zurich: Wichmann Press, 1997. 275～282

12 Ghidary S S, Tani T, Takamori T, Hattori M. A new home robot positioning system (HRPS) using IR switched multi ultrasonic sensors. IEEE International Conference on System, Man and Cybernetics, Tokyo: IEEE Press, 1999. 737～741

XU De Associate professor at Institute of Automation, Chinese Academy of Sciences. Received his bachelor and master degree from Shandong University of Technology in 1985 and 1990, respectively. He received his Ph. D. degree from Zhejiang University in 2001. His research interests include robot control, etc.

TAN Min Received his bachelor degree from Tsinghua University in 1986 and his Ph. D. degree from Institute of Automation, Chinese Academy of Sciences in 1990, respectively. His research interests include robot control, system reliability, etc.

移动机器人的在线实时定位研究

徐 德 谭 民

（中国科学院自动化研究所复杂系统与智能科学实验室 北京 100080）

（E-mail: xude@compsys.ia.ac.cn）

摘 要 对推算定位法进行了研究，提出了一种改进方案. 通过对移动机器人运动轨迹与状态的分析，导出了一类移动机器人的基于轨迹的运动学新模型. 利用移动机器人三个轮子的里程信息和导向轮的转角信息，通过信息模糊融合获得转弯半径和转角，再利用运动学模型获得机器人的位置和方向. 将这种改进的推算定位法与主动灯塔法相结合，提出了一种用于室内移动机器人的定位方法. 仿真结果表明，该方法具有实时性好、精度高、成本低、鲁棒性好等特点，并适用于不平整地面.

关键词 移动机器人，定位，运动学，模糊融合

中图分类号 TP24